The Cryosphere Discuss., https://doi.org/10.5194/tc-2017-242
Manuscript under review for journal The Cryosphere
Discussion started: 2 January 2018

The Cryosphere Discussions
Open Access
EGU

Basal drag of Fleming Glacier, Antarctica, Part B: implications of evolution from 2008 to 2015

Chen Zhao[1], Rupert M. Gladstone[2], Roland C. Warner[3], Matt A. King[1], Thomas Zwinger[4]

[1] School of Land and Food, University of Tasmania, Hobart, Australia
[2] Arctic Centre, University of Lapland, Rovaniemi, Finland
[3]Antarctic Climate and Ecosystems Cooperative Research Centre, University of Tasmania, Hobart, Australia
[4] CSC-IT Center for Science Ltd., Espoo, Finland

Abstract

The Wordie Ice Shelf-Fleming Glacier system in the southern Antarctic Peninsula has experienced a long-term retreat and disintegration of its ice shelf in the past 50 years. Upstream glacier acceleration and dynamic thinning have been observed over the past two decades, especially after 2008 when only a little constraining ice shelf remained at the Fleming Glacier front. It is important to know whether the substantial speed up and surface draw-down of the glacier since 2008 is a direct response to increasing ocean forcing or driven by the feedback within an unstable marine-based glacier system or both. To explore the mechanism underlying the changes, we use a Stokes (full stress) model to simulate the basal shear stress of the Fleming system in 2008 and 2015. Recent observational studies have suggested the 2008-2015 velocity change was due to the ungrounding of the Fleming Glacier front. Our modelling shows that the fast flowing region of the Fleming Glacier shows a very low basal shear stress in 2008 but with a band of higher basal shear stress along the ice front. It indicates that the ungrounding process might have not started in 2008, which is consistent with the height above buoyancy calculation in 2008. Comparison of our inversions for basal shear stresses for 2008 and 2015 suggests the migration of the grounding line by ~9 km upstream from the grounding line position in 1996, a shift which is consistent with the change in floating area deduced from the height above buoyancy in 2015. The southern branch of the Fleming Glacier and the Prospect Glacier apparently have retreated by ~1-3 km from 2008 to 2015. The retrograde bed underneath the Fleming Glacier has promoted migration of the grounding line, which we suggest may be triggered by subglacial drainage as a response to the increased basal water supply through greater frictional heating at the ice-bedrock interface further upstream in the fast-flowing region. Improved knowledge of bed topography near the grounding line and further transient simulation is required to predict the future grounding line movement of the Fleming Glacier system precisely and subsequently understand better the ice dynamics and the its future contribution to sea level.

1 Introduction

In the past few decades, glaciers in West Antarctica and the Antarctic Peninsula (AP) have experienced rapid regional atmospheric and oceanic warming, leading to significant retreat and disintegration of ice shelves and rapid acceleration of mass discharge and dynamic thinning of their feeding glaciers (Cook et al., 2016; Gardner et al., 2017; Wouters et al., 2015). Most of the West Antarctic Ice Sheet and the glaciated margins of the AP (Fig. 1a) rest on a bed below sea level sloping down towards the ice sheet interior, and the grounding lines of outlet glaciers located on such reverse bed slopes may be vulnerable to rapid retreat depending on the bedrock and ice shelf geometry (e.g., Gudmundsson (2013); Gudmundsson et al. (2012); Schoof (2007)). Once perturbed past a critical threshold, such as grounding-line retreat over a bedrock hump into a region of retrograde slope, the GL will continue to retreat

The Cryosphere Discuss., https://doi.org/10.5194/tc-2017-242
Manuscript under review for journal The Cryosphere
Discussion started: 2 January 2018

inward until the next stable state without any additional external forcing. This marine ice sheet instability has been invoked to explain the recent widespread and rapid grounding line retreat of glaciers in the Amundsen Sea sector, possibly driven by increased basal melting reducing the buttressing influence of ice shelves (Rignot et al., 2014). Rapid grounding line retreat and accelerated flow in these unstable systems leads to significant increases in ice flux and increased contribution from these marine ice sheets to sea-level rise.

The former Wordie Ice Shelf (WIS; Fig. 1b) in the western coast of AP started its initial recession in 1960s with a substantial break-up occurring around 1989, followed by continuous steady retreat (Cook and Vaughan, 2010; Vaughan and Doake, 1996; Zhao et al., 2017). The former ice shelf is fed by three tributaries as shown in Fig. 1b. The Fleming Glacier (FGL; Fig. 1b), as the main tributary glacier, splits into two branches: the main branch to the north and the southern branch (hereafter "southern FGL"). The floating part in front of the main FGL nearly disappeared sometime between 1997 and 2000 (Fig. 1b), and the ice front position in 2008 almost coincides with the latest known grounding line position in 1996 (Rignot et al., 2011a). The main branch of the FGL has thinned at a rate of -6.25±0.20 m yr^{-1} near the front from 2008 to 2015, nearly twice the thinning rate during 2002-2008 (-2.77±0.89 m yr^{-1}) (Zhao et al., 2017). This is consistent with the recent findings that the largest velocity changes across the whole Antarctic Ice Sheet over 2008-2015 occurred at FGL (500 m yr^{-1} increase close to the grounding line) (Walker and Gardner, 2017).

As a marine-type glacier system residing on a retrograde bed with bedrock as much as ~800 m below sea level (Fig. 1c), and hence potentially vulnerable to marine ice sheet instability, the acceleration and dynamic thinning of the FGL may indicate the onset of unstable rapid grounding line retreat (Friedl et al., 2017; Walker and Gardner, 2017; Zhao et al., 2017). The speedup of the FGL before 2008 was originally assumed to be a direct response to the loss of buttressing due to the ice shelf collapse (Rignot et al., 2005; Wendt et al., 2010). Recent studies have suggested that the recent speedup and retreat could be a direct response to oceanic forcing (Friedl et al., 2017; Walker and Gardner, 2017). None of the past studies have modelled the glacier system and hence these hypotheses are untested. In this paper we explore the potential for these hypotheses in Sect. 5.

By analyzing the detailed history of surface velocities and rates of elevation change from 1994 to 2016, Friedl et al. (2017) showed that the initial ungrounding of the FGL from the 1996 grounding line position (Rignot et al., 2011a) occurred in 2008 and further expanded upstream by ~6-9 km from 2011 to 2014, which explained the speedup of the FGL since 2008, and they speculated this was mainly caused by the increased basal melting at the grounding line due to the upwelling of the warm Circumpolar Deep Water (CDW). However, this study lacked direct measurements of basal melting and did not perform relevant numerical modeling, so it is still uncertain whether the enhanced basal melting triggered by ocean warming is the dominant reason for the ungrounding process.

Subglacial melting occurring at the ice-bed interface away from the grounding line could be another possible factor in the glacier acceleration owing to a positive feedback between the basal sliding and subglacial melt water volume (Bartholomaus et al., 2008; Schoof, 2010).

Changes in basal shear stress connected with changes in glacier flow could reveal the possible movement of the grounding line and also indicate possible influences on the changing dynamics. In this study, we employed the Elmer/Ice code (http://elmerice.elmerfem.org/) (Gagliardini et al., 2013), a new generation three-dimensional (3D) full-Stokes ice sheet model, to solve the Stokes equations over the whole WIS-FGL catchment. Our implementation of the model solves the ice flow equations and the steady-state heat equation (Gagliardini et al., 2013; Gladstone et al., 2014). We also infer the basal shear stress using control inverse methods (e.g., Gillet-Chaulet et al. (2016); Gladstone et al. (2017); Gong et al. (2016)).

In first part of this study (Zhao et al., companion paper), we explored the sensitivity of the inversion for basal shear stress to initial assumptions about englacial temperatures, bed

elevation data, and ice front boundary condition. In this second part of this study (the current paper), we adopt the three-cycle spin-up scheme of Zhao et al. (companion paper) to derive the distributions of basal shear stress in 2008 and 2015. We present the observational data in Sect. 2 and our methods in Sect. 3. We compare the resulting basal shear distributions for the 2008 and 2015 and their connections with driving stress and basal friction heating in Sect. 4.1 and Sect. 4.2. The height above buoyancy for the two epochs is computed in Sect. 4.3 as an independent guide to grounding line changes. Through comparison of basal shear stress and height above buoyancy between 2008 and 2015, we analyze the stability of the grounding line in this period and discuss ongoing marine ice sheet instability and direct oceanic forcing as possible reasons for the sharp speed-up of the FGL in Sect. 5.

2 Observational Data

2.1 Surface elevation data in 2008 and 2015

The surface elevation data for 2008 (DEM2008; Fig. 2a) from Zhao et al. (companion paper) was used here. To estimate the surface topography in 2015 (DEM2015; Fig. 2a), we generated the average surface-lowering rate during 2008-2015 for the fast flow regions (surface velocity in 2008 $\geq$ 20 m yr^{-1}) by using the hypsometric model for elevation change described in Zhao et al. (2017) during the same period. The DEM2015 was then generated from the DEM2008 applying the ice thinning rates from 2008 to 2015. For the area with velocities < 20 m yr^{-1}, we assume the DEM in 2015 remains the same as that in 2008.

2.2 Bed elevation data

The bed topography plays a significant role in simulation of basal sliding and ice flow distribution for fast-flowing glaciers (Zhao et al., companion paper), and also in interpreting the grounding line movement precisely (De Rydt et al., 2013; Durand et al., 2011; Rignot et al., 2014). Zhao et al. (companion paper) discussed the sensitivity of the basal shear stress distribution to three bedrock topography datasets, and bed_zc (Fig. 2b) with high accuracy and resolution, was suggested as the most suitable bedrock data for modeling the WIS-FGL system. Here bed_zc is computed by:

$$bed\_zc = S_{2008} - H_{mc} \quad (1)$$

where S_{2008} is the surface DEM in 2008, and H_{mc} is the ice thickness data with a resolution of 450 m combined from the Center for Remote Sensing of Ice Sheets (CReSIS) ice thickness measurements using a mass conservation method for the regions of fast flow (Morlighem et al., 2011; Morlighem et al., 2013), and ice thickness from Bedmap2 (Fretwell et al., 2013).

2.3 Surface velocity data in 2008 and 2015

We use the same velocity data for 2008 as in Part 1 of this study (Zhao et al., companion paper), which is from InSAR-based Antarctic ice velocity (MEaSUREs version 1.0) produced from the fall 2007 and/or 2008 by Rignot et al. (2011b). The 2008 velocity has a resolution of 900 m and the uncertainties over the study region ranges from 4 m yr^{-1} to 8 m yr^{-1} over the study area. For 2015, we adopt the velocity data extracted from Landsat 8 imagery with a resolution of 240 m and errors ranging from 5 m yr^{-1} to 20 m yr^{-1} (Gardner et al., 2017). Velocity data in 2015 has a full coverage over the WIS-FGL domain, while the velocity in 2008 has no data in the gray area in Fig. 1b.

2.4 Other datasets

The temperature field is simulated with a linear initial temperature, which does not affect the final inversion results as demonstrated in Zhao et al. (companion paper). The surface

The Cryosphere Discuss., https://doi.org/10.5194/tc-2017-242
Manuscript under review for journal The Cryosphere
Discussion started: 2 January 2018

temperature is constrained by yearly averaged surface temperature over 1979-2014 computed from RACMO2.3/ANT27 (van Wessem et al., 2014) and the bottom heat flux boundary condition includes the geothermal heat flux from Fox Maule et al. (2005) and the simulated basal frictional heating.

Our DEM is an ellipsoidal WGS84 system and hence a height of 0 m does not refer to sea level. An observed sea level height of 15 m (WGS84 ellipsoidal height) in Marguerite Bay (Zhao et al., companion paper) was taken to compute the sea pressure on the ice front.

3 Method

The modeling method using Elmer/Ice presented in Part 1 of this study (Zhao et al., companion paper) is adopted here, including the mesh generation, mesh refinement, and applied boundary conditions. The simulations for the two epochs retain the same assumptions about the ice-covered domain, namely a common spatial extent with fixed ice front location, and the assumption that all the ice is grounded.

We follow the three-cycle spin-up scheme (Zhao et al., companion paper) and simulate the basal shear stress τ_b in 2008 and 2015 with the linear sliding law:

$$\tau_b = C u_b \tag{2}$$

Here C is a basal drag coefficient and u_b is the basal sliding velocity.

There are two key differences between the data used for the 2008 and 2015 inversions: increased surface velocity and changed ice geometry, namely a thinner glacier in 2015 compared to 2008 due to dynamic thinning. To explore their relative impacts, we carry out an additional inversion with the geometry from 2008 but the surface velocity from 2015 (see Appendix A). We found that both geometry variations and velocity changes are important to the inverted basal stress condition.

To explore the relationship between the basal shear stress and local gravitational driving stress τ_d, the gravitational driving stress is also computed for both epochs:

$$\tau_d = \rho_i g H \left|\vec{\nabla} z_s\right| \tag{3}$$

where ρ_i is the ice density, H is the ice thickness, and $\left|\vec{\nabla} z_s\right|$ is the gradient of the ice surface. Considering the snow and firn on the ice surface, we apply a relatively low ice density of 900 kg m^{-3} following Berthier et al. (2012).

Subglacial water has the capacity to modulate ice velocity and mass balance for outlet glaciers (Bell, 2008; Sergienko et al., 2014). To explore the possible flow path of subglacial water beneath the FGL, we calculate hydraulic potential at the bed, and the gradient of this governs subglacial flow. The hydraulic potential (Φ), expressed in equivalent metres of water, is given by:

$$\Phi = (z_s - z_b)\frac{\rho_i}{\rho_{fw}} + z_b \tag{4}$$

where ρ_{fw} is the fresh water density (1000 kg m^{-3}), z_s and z_b are the surface and bed elevations, respectively.

Height above buoyancy (Z_*) is a good indicator of how heavily grounded a glacier is, which is relevant to the glacier's evolution and additionally helps interpret the likely floating regions based on simulated basal shear stress in this study. Z_* is related to the effective pressure N at the bed by the relationship:

$$N = \rho_i g Z_* \tag{5}$$

In this study, we use a simpler hydrostatic balance based on sea level with the relationship:

The Cryosphere Discuss., https://doi.org/10.5194/tc-2017-242
Manuscript under review for journal The Cryosphere
Discussion started: 2 January 2018

$$Z_* = \begin{cases} H, & if\ z_b >= z_{sl} \\ H + (z_b - z_{sl})\frac{\rho_w}{\rho_i}, & if\ z_b < z_{sl} \end{cases} \quad (6)$$

where z_{sl} is the sea level.

4 Results

4.1 Comparison of basal shear stress and driving stress in 2008 and 2015

We obtain the spatial distributions for basal shear stress, τ_b (Figs. 3a, 3b), and basal velocity of the WIS-FGL system for 2008 and 2015 using the inversion method to determine the basal drag coefficient, $\boldsymbol{C}$, with the geometry and velocity data described above. In 2008 the main FGL shows a band of high basal shear stress approximately 2 km wide along the ice front (Fig. 3a), while immediately upstream a region of low basal stress covers most of the downstream bedrock basin, returning to more typical values ~9 km from the ice front. In contrast, the basal drag at the front of the southern FGL is low, with more typical values ~2 km upstream. By 2015, the high drag band near the FGL ice front has disappeared while in the downstream basin the already low basal drag seen in 2008 is even lower in 2015 (Fig. 3b), which is consistent with observed speed-up from 2008 to 2015. Further upstream in the basin, including the ridge between the downstream and upstream basins, the basal shear stress does not change much between the two epochs. To explore the ice dynamics evolution from 2008 to 2015, we present the ratio of basal shear stress τ_b to driving stress τ_d (hereafter referred as "RBD") in Figs. 3c, 3d, which can provide insight into the dynamical regime (Sergienko et al., 2014). In particular, it provides an indication whether the driving stress is locally balanced by the basal shear or whether there is a significant role for membrane stresses and a regional momentum balance. We assume the region with τ_b < 0.01 MPa or RBD < 0.1 to be the low drag area considering the uncertainties of the model input, and the very low inferred basal drag is assumed to correspond to flotation.

It is hard to determine whether the high basal shear stress band detected at the front of the main branch of the FGL in 2008 (Fig. 3a) is a real feature or at least in part an artifact error due to uncertainties from the ice thickness, local bed topography, local sea level, and the ice front position. Sensitivity to such uncertainties was explored in Zhao et al. (companion paper), and the adjustment of ice front boundary condition with a higher sea level of 25 m shows decrease in the basal shear stress around the ice front but has not shown any sign of disappearance of the high basal drag band. Improved bed topography data and accurate ice front position are necessary to interpret the precise grounding line position in 2008.

As expected, the gravitational driving stress of this system shows no significant changes from 2008 (Fig. 3e) to 2015 (Fig. 3f). In 2015, the boundaries of the zone in the main FGL with τ_{b2015} < 0.01 MPa (magenta lines in Fig. 3b and Fig. 4) or RBD_{2015} < 0.1 (red lines in Fig. 3d and Fig. 4) are partly consistent with the deduced grounding line position of the FGL in 2015 (Friedl et al., 2017) (white dots in Figs. 3 and 4). The differences with that study are around the northern and eastern parts, but the magenta and red boundaries (Figs. 4c, 4d) in the northern part fit the bedrock ridges in this study, while the white points fit the corresponding bedrock topography data in Friedl et al. (2017). This result confirms the significant role of bedrock topography in determining the grounding line position. Around the eastern part of the region within which velocities > 1500 m yr^{-1} (cyan contour in Fig. 3b), the low basal drag area in this study extends ~1-3 km further upstream than the extracted grounding line in 2015 (Friedl et al., 2017). An unexplained rib-like basal resistance pattern (τ_{b_2015} > 0.1 MPa) is found approaching the Fleming front parallel to the yellow velocity contour (Fig. 3b). This feature, which is not present in 2008 (Fig. 3a), is located within the boundary area from topographic low to high along the southern margin of the downstream FGL (Fig. 4d).

The Cryosphere Discuss., https://doi.org/10.5194/tc-2017-242
Manuscript under review for journal The Cryosphere
Discussion started: 2 January 2018

Comparison of basal shear stress between 2008 (Fig. 3a) and 2015 (Fig. 3b) shows a significant decrease from 2008 to 2015 in fast flowing regions (velocity > 1500 m yr^{-1}) at the front of the FGL. A similar pattern occurred at front of the PGL and the southern FGL. For the southern FGL, the grounding line has retreated by ~2 km in 2008 from the last known grounding line position in 1996 (Rignot et al., 2011a) (Fig. 3a) and continued retreating by ~3 km upstream in 2015 (Fig. 3b). For the PGL, the grounding line in 2008 largely coincides with that in 1996 (Fig. 3a) but retreats by ~3 km until 2015 (Fig. 3b). We attribute this decreased basal friction to the ice ungrounding process from 2008 to 2015.

4.2 Basal melting and subglacial hydrology

Subglacial water could be a contributor to low basal shear stress and high basal sliding at the base of the FGL. It arises from two main sources in polar regions: either surface melt water draining into the subglacial hydrologic system via crevasses or moulins or in-situ melting at the bed (Banwell et al., 2016; Dunse et al., 2015; Hoffman and Price, 2014). Hoffman and Price (2014) also found a positive feedback between the basal melt and basal sliding through the frictional heating on an idealized mountain glacier using coupled subglacial hydrology and ice dynamics models. However, the amount of surface melt water in this region is not thought to be sufficient to percolate to the base (Rignot et al., 2005), so we take basal melting due to the friction heat and geothermal heat flux as the only source of subglacial water. Geothermal heat flux at the fast flowing regions of our study area (Fox Maule et al., 2005) is two orders of magnitude smaller than the friction heating at the base, leaving friction heating as the dominant factor in generating basal melt water.

To explore the potential subglacial water sources and likely flow directions, we plot the frictional heating (Figs. 4a, 4b), the contours of hydraulic potential (Φ) (Figs. 4c, 4d), and the basal homologous temperature (temperature relative to the melting point) (Figs. 4e, 4f) in both epochs. Friction heating due to sliding at the bed (Figs. 4a, 4b) provides a basal melt water source where ice is at pressure melting temperature, which is the case for the fast flow regions of the FGL (see the basal homologous temperature in Figs. 4e, 4f), and the gradient of the hydraulic potential (Figs. 4c, 4d) indicates likely water flow paths at the ice-bed interface. The frictional heat generated at the base is high where both basal shear stress and basal sliding velocities are high. The modeled friction heating in both 2008 and 2015 (Figs. 4a, 4b) extends as far and high as in the upstream basin under the FGL, indicating high basal melt rates in this region (a heat flux of 1 W m^{-2} could melt ice at the rate of 0.1 m yr^{-1} in regions at the pressure melting temperature). The highest friction heating is generated over the bedrock rise between the FGL upstream and downstream basins, where the most melt water will be generated and will be routed towards the downstream basin given the gradient of hydraulic potential in this region (Figs. 4c, 4d). Hence it is a major source of basal water for the downstream basin. This could explain the low basal drag downstream, while the increase in heating between 2008 and 2015 could further enhance the basal sliding in fast-flowing regions. Both the hydraulic potential and frictional heating could help to understand the mechanism behind the rapid acceleration and surface draw-down of the FGL, which is further discussed in Sect. 5.

4.3 Height above buoyancy Z_*

We compute Z_* for 2008 and 2015 for the FGL based on Eq. (6) with a sea level of 15 m (Figs. 5a, 5b). To allow for the over- or underestimation of Z_* owing to uncertainties from the topography data, ice thickness, ice density and the sea level applied above, we suggest that the areas where $|Z_*| < 20$ m might be floating, and accordingly include areas where $Z_* > -20$ m in Fig. 5.

A low height above buoyancy Z_* in 2008 (Fig. 5a) is only found near the 1996 grounding line position in the downstream basin, which reveals that ungrounding of the main FGL may not have started or only just commenced in 2008. In 2015, the area close to flotation with $Z_* < 20$

The Cryosphere Discuss., https://doi.org/10.5194/tc-2017-242
Manuscript under review for journal The Cryosphere
Discussion started: 2 January 2018

m (taken as an upper limit) has expanded about 9 km upstream in 2015 (magenta lines in Fig. 5b), which broadly coincides with the estimated grounding line in 2015 (Friedl et al., 2017) except for an almost encircled patch with slightly higher Z_* (20-30 m). The implications of different Z_* from 2008 and 2015 are a small FGL grounding line retreat from 1996 to 2008 but significant retreat from 2008 to 2015. Uncertainty in the predicted grounding line in 2015 is significant, but a new position ~9 km upstream is likely.

In addition to the main branch of the FGL, its southern branch and the PGL also show a reduction in Z_*, which suggests grounding line retreat. Based on the area with $Z_* < 20$ m, the southern FGL has retreated by ~1.5 km between 1996 and 2008 (Fig. 5a) and a further ~1-1.5 km by 2015, with an associated increase in floating area (Fig. 5b). The PGL does not show obvious sign of retreat between 1996 and 2008 but migrates for ~1 km upstream by 2015.

Changes in Z_* from 2008 to 2015 suggest an ungrounded area consistent with the area of very low modelled basal shear stress shown in Figs. 3a and 3b. The area close to floating, defined by $Z_* < 20$ m, constitutes additional evidence supporting the rapid grounding line retreat over 2008 to 2015 and the likely grounding line positions in both epochs.

5 Discussions

A band of high basal shear stress near the terminus of the FGL in 2008 suggests that the ice front might have been still grounded at that time, an interpretation consistent with the relatively high bedrock topography near the ice front compared to upstream. Friedl et al. (2017) deduced the likely grounding line position of the FGL in 2008 at a possible small hill from the bedrock topography (~2.5 km upstream of the 1996 grounding line) as the interpretation of rapid surface acceleration detected around March-April 2008. The acceleration phase in March-April 2008 occurred later than the timing of the DEM2008 data used in this study (acquired in January 2008 for fast-flowing regions). Therefore it is quite possible that the grounding line had not retreated by January 2008. The analysis of height above buoyancy for the DEM2008 supports the main FGL being grounded close to the ice front and hence near the 1996 location. Considering the uncertainties of grounding line position in 1996 (several kilometers) (Rignot et al., 2011a) and uncertainty about interpreting the frontal high basal drag band in this study, the exact grounding line position in January 2008 is somewhat uncertain, as is the extent of any retreat associated with the significant acceleration during March-April 2008 (Friedl et al., 2017).

The disappearance of a high basal resistance band (a likely physical pinning band) near the FGL front between 2008 and 2015 is a likely trigger for the sudden acceleration and increased surface lowering of the FGL. The increased flux of ice, combined with the glacier geometry, suggests the substantial grounding line retreat, which agrees with two recent studies (Friedl et al., 2017; Walker and Gardner, 2017). The timing of these accelerations suggests that the loss of this basal resistance occurred shortly after the epoch we analyzed (Jan 2008). Given the low basal drag already present over most of the downstream basin one would expect the loss of the localized drag near the ice front to promptly result in an increase in velocity over the entire low-drag region. This is consistent with the near uniform increase in velocity reported in early 2008 by Friedl et al. (2017) for a region 4-10 km upstream of the 1996 grounding line.

For a glacier lying on a retrograde slope in a deep trough, the grounding line may be vulnerable to rapid retreat without any further change in external forcing once its geometry crosses a critical threshold (e.g. due to detachment from a pinning point), as in the rapid retreat of Jakobshavn Isbræ in West Greenland (Steiger et al., 2017). The grounding line in 2008 may have experienced a retreat after moving across the geometric pinning band near the front, and then retreated further to the position in 2015 about 9 km upstream in the FGL downstream basin. A similar ungrounding process has been detected in the Thwaites, Smith and Pine Island Glaciers from 1996 to 2011 (Rignot et al., 2014).

The Cryosphere Discuss., https://doi.org/10.5194/tc-2017-242
Manuscript under review for journal The Cryosphere
Discussion started: 2 January 2018

The current grounding line of the FGL appears to be on the prograde slope of the bedrock high between the FGL downstream and upstream basins. With the establishment of an ocean cavity under the new ice shelf we can expect that ocean driven basal melting will further modify the thickness of the recently ungrounded ice. If the system remains out of balance and continues to thin, the grounding line could eventually move across this bed obstacle and the grounding line is likely to retreat rapidly down the retrograde face of the FGL upstream basin, accompanied by further glacier speed up and dynamic thinning, unless the ice shelf buttressing of an increasingly long and confined fjord-like Fleming ice shelf increases sufficiently to restore its stability (Gudmundsson, 2013).

Walker and Gardner (2017) attribute the sharp increase in observed ice velocity and drop in surface elevation from 2008 to 2015 to increased calving front melting caused by incursion of relatively warm Circumpolar Deep Water (CDW). The CDW flows onto the continental shelf within the Bellingshausen Sea, penetrating into the Marguerite Bay, driven by changes in regional wind patterns resulting from global atmospheric circulation changes (Walker and Gardner, 2017). Friedl et al. (2017) also explain the landward migration of the grounding line with the same mechanism, namely the increased front and/or basal melting due to ocean warming. This explanation appears consistent with the finding that the acceleration, retreat, and thinning of outlet glaciers in the Amundsen Sea Embayment (ASE) are triggered by the ungrounding process due to the inflow of warm CDW onto its continental shelf and into sub-ice-shelf cavities (Turner et al., 2017). However, the floating parts of the FGL remained negligible in 2008 based on the height above buoyancy in 2008 (Fig. 5a). The speedup and ungrounding occurring in the ASE glaciers was a direct response to significant loss of buttressing caused by ice shelf thinning and grounding-line retreat (Turner et al., 2017). When the CDW incursions started in the ASE, the floating parts of ASE glaciers were much larger than the residual ice shelf of the Fleming system in 2008. After the recent changes the newly floating region of the FGL has an area of ~60 km^2, based on the estimated 2015 grounding line from Friedl et al. (2017) and the 2016 ice front position in this study. Our height above buoyancy analysis for 2015 (Fig. 5b) also indicates substantial grounding line retreat since 2008. So, significant buttressing reduction is not likely to have occurred on the FGL during the rapid acceleration of 2008, but further changes to the FGL after 2015 may resemble ASE glacier and ice shelf systems more closely. No direct measurements are available to confirm the direct effect of the frontal or basal melting on the FGL grounding zone over this period, nor have previous studies attempted to quantify the amount of melting required to drive significant FGL grounding line retreat. The ocean-driven basal melting at the ice shelf front or base may have contributed to grounding line retreat, or the reduction of the frontal high basal shear zone, but establishing this as the main cause would require further quantification of the cause-effect link.

Ongoing presence of subglacial water could contribute to a radical destabilization of marine ice sheet systems. Evidence suggests that increased basal water supply could accelerate basal motion and surface lowering of both mountain glaciers (Bartholomaus et al., 2008) and ice sheets (Hoffman et al., 2011), and further contribute to grounding line retreat of marine-based glaciers. Jenkins (2011) has also suggested that subglacial water emerging at the grounding line can enhance local ice shelf basal melt rates by driving buoyancy driven plumes in the ocean cavity. The rapid sliding and high friction heating in the upstream FGL (Figs. 4a, 4b) has provided evidence for an extensive active hydrologic system beneath the FGL.

High frictionally-generated heat in the upstream basin of the FGL is the main source of meltwater flowing into the FGL downstream basin. It is also clear that the frictional heating in 2015 (Fig. 4b) is greater than in 2008 in the upstream basin (Fig. 4a), indicating more basal melt water generation in 2015. The plateau in hydraulic potential in the upstream basin of the FGL suggests the possibility that basal water may accumulate in this region, or at least show a low throughput. This plateau appears to be fed by an extensive upstream region with a large frictional heat source. Outflow from this plateau region, according to our hydraulic potential calculations, is likely to be predominantly in the direction of the downstream basin, but future

outflow across the shallow saddle in hydraulic potential towards the Southern branch cannot be ruled out, since the evolution of the potential responds to the changing elevation, as can be seen by comparing the contours in Figs. 4c and 4d.

The further sharp speed-up events that occurred in 2010-2011 reported by Friedl et al. (2017) have several potential causes in addition to the previously proposed mechanism of a direct response to ocean-induced melting (Walker and Gardner, 2017). One possibility is an outburst of subglacial water from the upstream basin after subglacial water building up over years to decades in response to increased sliding and friction heating and progressive lowering of the ice surface. Another possibility is local unpinning near the retreating grounding line: ungrounding from pinning points may cause a step reduction in basal resistance. Another possibility could be positive feedbacks in the subglacial hydrologic system – rapid change may result from the direct feedback between sliding speed, friction heat and basal water.

The height above buoyancy is an indicator for the vulnerability of marine-based grounded ice to dynamic thinning and acceleration. The area with $Z_* < 20$ m in 2015 has shown that the downstream basin is currently ungrounding and this may continue until the grounding line finds a stable position on the prograde slope separating the two major basins. More thinning would be needed to destabilise the upstream basin, and it is hard to say how much forcing would be needed to push the grounding line into it. If the retrograde slope of the upstream basin is reached, further rapid and extensive grounding line retreat would be expected. A clear decrease can be seen in Z_* from 2008 (red in Fig. 5a) to 2015 (dark red in Fig. 5b) in the upstream basin (around the 2015 velocity contour of 1000 m yr^{-1}), indicating the potential vulnerability of the FGL to continued ice mass loss. The surface lowering rate between 2008 and 2015 in this region is ~6 m yr^{-1} (Zhao et al., 2017). If this thinning trend continues linearly with time, the ice in regions with Z_* of 200-300 m would be expected to unground in ~30-50 years. This could be longer or shorter if the thinning rate is not linear with time.

In the absence of precise and accurate knowledge of bed topography and ice shelf/stream basal processes, the dominant cause of ungrounding cannot be determined. Further research is necessary to better understand the dominant mechanisms.

6 Conclusions

We used a Stokes solver (Elmer/Ice) to simulate the basal shear stress, temperature and frictional heating of the Wordie Ice Shelf-Fleming Glacier system in 2008 and 2015. Both increased surface velocity and surface lowering during this period are important for the calculation of basal shear stress.

Decreased basal drag from 2008 to 2015 in the Fleming Glacier downstream basin indicates significant grounding line retreat, consistent with change in suggested floating area based on the geometry in 2015 and the deduced grounding line in 2015 (Friedl et al., 2017). Grounding line retreat also occurred on the southern branch of the FGL and the PGL. Our height above buoyancy calculations also indicate the FGL downstream basin was close to flotation in 2015 and is vulnerable to continued ice thinning and acceleration.

Pronounced basal melting driven by oceanic warming in the Marguerite Bay may have contributed to the ungrounding of the Fleming Glacier front in 2008, as previously suggested by Walker and Gardner (2017) and Friedl et al. (2017), but feedbacks in the subglacial hydrologic system may provide the dominant trigger for rapid increases in basal sliding and ungrounding process. The derived basal shear distributions suggest a major influence was the loss of a narrow band of higher basal shear near the ice front of the main Fleming Glacier, as basal friction under most of the region considered afloat by 2015 was already low in 2008.

The marine-based portion of the Fleming Glacier extends far inland. It is not clear whether grounding line retreat into the Fleming Glacier upstream basin will occur. Transient simulations with improved knowledge of bed topography are necessary to predict the

movement of the grounding line and how long it will take to achieve a new stable state. Coupled ice sheet ocean modelling may be required to explore the evolution of the new ice shelf. Future studies of the dynamic evolution of Fleming Glacier will enhance our understanding of its vulnerability to marine ice sheet instability and provide projections of its future behavior.

Appendix A: Sensitivity to velocity changes

Figure A1 shows the results from the inversion for basal shear stress in 2008 (Fig. A1a), 2015 (Fig. A1b), and from another additional inversion with the geometry from 2008 but using surface velocity from 2015 (Fig. A1c). The basal shear stress of this hybrid simulation shows patterns and magnitudes between those of the standard 2008 and 2015 simulations. This suggests that changes in both ice geometry and velocities have comparable impact on the inferred basal shear stress distribution, with the implication that an inversion study based on a change in either velocity or geometry alone would underestimate the change in basal drag.

Author Contribution

Chen Zhao collected the datasets, ran the simulation, and drafted the paper. All authors contributed to the refinement of the experiments, the interpretation of the results and the final manuscript.

Acknowledgements

Chen Zhao is a recipient of an Australian Government Research Training Program Scholarship and Quantitative Antarctic Science Program Top-up Scholarship. Rupert Gladstone is funded by the European Union Seventh Framework Program (FP7/2007-2013) under grant agreement number 299035 and by Academy of Finland grant number 286587. Matt A. King is a recipient of an Australian Research Council Future Fellowship (project number FT110100207) and is supported by the Australian Research Council Special Research Initiative for Antarctic Gateway Partnership (Project ID SR140300001). Thomas Zwinger's contribution has been covered by the Academy of Finland grant number 286587. This work was supported by the Australian Government's Business Cooperative Research Centres Programme through the Antarctic Climate and Ecosystems Cooperative Research Centre (ACE CRC). This research was undertaken with the assistance of resources and services from the National Computational Infrastructure (NCI), which is supported by the Australian Government. We thank Alex S. Gardner for providing the velocity dataset for 2015 and Mathieu Morlighem for the ice thickness data. We thank E. Rignot, J. Mouginot, and B. Scheuchl for making their SAR velocities publically available. We thank Yongmei Gong for advice on the analysis of hydraulic potential. SPOT 5 images and DEMs were provided by the International Polar Year SPIRIT project (Korona et al., 2009), funded by the French Space Agency (CNES). This work is based on data services provided by the UNAVCO Facility with support from the National Science Foundation (NSF) and National Aeronautics and Space Administration (NASA) under NSF Cooperative Agreement No. EAR-0735156. The ASTER L1T data product was retrieved from https://lpdaac.usgs.gov/data_access/data_pool, maintained by the NASA EOSDIS Land Processes Distributed Active Archive Center (LP DAAC) at the USGS/Earth Resources Observation and Science (EROS) Center, Sioux Falls, South Dakota.

Reference

Banwell, A., Hewitt, I., Willis, I., and Arnold, N.: Moulin density controls drainage development beneath the Greenland ice sheet, Journal of Geophysical Research: Earth Surface, 121, 2248-2269, 2016.

Bartholomaus, T. C., Anderson, R. S., and Anderson, S. P.: Response of glacier basal motion to transient water storage, Nature Geosci, 1, 33-37, 2008.

Bell, R. E.: The role of subglacial water in ice-sheet mass balance, Nature Geosci, 1, 297-304, 2008.

Berthier, E., Scambos, T. A., and Shuman, C. A.: Mass loss of Larsen B tributary glaciers (Antarctic Peninsula) unabated since 2002, Geophysical Research Letters, 39, 2012.

Cook, A. J., Holland, P. R., Meredith, M. P., Murray, T., Luckman, A., and Vaughan, D. G.: Ocean forcing of glacier retreat in the western Antarctic Peninsula, Science, 353, 283-286, 2016.

Cook, A. J. and Vaughan, D. G.: Overview of areal changes of the ice shelves on the Antarctic Peninsula over the past 50 years, The Cryosphere, 4, 77-98, 2010.

De Rydt, J., Gudmundsson, G. H., Corr, H. F. J., and Christoffersen, P.: Surface undulations of Antarctic ice streams tightly controlled by bedrock topography, The Cryosphere, 7, 407-417, 2013.

Dunse, T., Schellenberger, T., Hagen, J. O., Kääb, A., Schuler, T. V., and Reijmer, C. H.: Glacier-surge mechanisms promoted by a hydro-thermodynamic feedback to summer melt, The Cryosphere, 9, 197-215, 2015.

Durand, G., Gagliardini, O., Favier, L., Zwinger, T., and le Meur, E.: Impact of bedrock description on modeling ice sheet dynamics, Geophysical Research Letters, 38, n/a-n/a, 2011.

Fox Maule, C., Purucker, M. E., Olsen, N., and Mosegaard, K.: Heat Flux Anomalies in Antarctica Revealed by Satellite Magnetic Data, Science, 309, 464-467, 2005.

Fretwell, P., Pritchard, H. D., Vaughan, D. G., Bamber, J. L., Barrand, N. E., Bell, R., Bianchi, C., Bingham, R. G., Blankenship, D. D., Casassa, G., Catania, G., Callens, D., Conway, H., Cook, A. J., Corr, H. F. J., Damaske, D., Damm, V., Ferraccioli, F., Forsberg, R., Fujita, S., Gim, Y., Gogineni, P., Griggs, J. A., Hindmarsh, R. C. A., Holmlund, P., Holt, J. W., Jacobel, R. W., Jenkins, A., Jokat, W., Jordan, T., King, E. C., Kohler, J., Krabill, W., Riger-Kusk, M., Langley, K. A., Leitchenkov, G., Leuschen, C., Luyendyk, B. P., Matsuoka, K., Mouginot, J., Nitsche, F. O., Nogi, Y., Nost, O. A., Popov, S. V., Rignot, E., Rippin, D. M., Rivera, A., Roberts, J., Ross, N., Siegert, M. J., Smith, A. M., Steinhage, D., Studinger, M., Sun, B., Tinto, B. K., Welch, B. C., Wilson, D., Young, D. A., Xiangbin, C., and Zirizzotti, A.: Bedmap2: improved ice bed, surface and thickness datasets for Antarctica, The Cryosphere, 7, 375-393, 2013.

Friedl, P., Seehaus, T. C., Wendt, A., Braun, M. H., and Höppner, K.: Recent dynamic changes on Fleming Glacier after the disintegration of Wordie Ice Shelf, Antarctic Peninsula, The Cryosphere Discuss., 2017, 1-26, 2017.

Gagliardini, O., Zwinger, T., Gillet-Chaulet, F., Durand, G., Favier, L., de Fleurian, B., Greve, R., Malinen, M., Martín, C., Råback, P., Ruokolainen, J., Sacchettini, M., Schäfer, M., Seddik, H., and Thies, J.: Capabilities and performance of Elmer/Ice, a new-generation ice sheet model, Geosci. Model Dev., 6, 1299-1318, 2013.

Gardner, A. S., Moholdt, G., Scambos, T., Fahnstock, M., Ligtenberg, S., van den Broeke, M., and Nilsson, J.: Increased West Antarctic ice discharge and East Antarctic stability over the last seven years, The Cryosphere Discuss., 2017, 1-39, 2017.

Gillet-Chaulet, F., Durand, G., Gagliardini, O., Mosbeux, C., Mouginot, J., Rémy, F., and Ritz, C.: Assimilation of surface velocities acquired between 1996 and 2010 to constrain the form of the basal friction law under Pine Island Glacier, Geophysical Research Letters, doi: 10.1002/2016GL069937, 2016. n/a-n/a, 2016.

Gladstone, R., Schäfer, M., Zwinger, T., Gong, Y., Strozzi, T., Mottram, R., Boberg, F., and Moore, J. C.: Importance of basal processes in simulations of a surging Svalbard outlet glacier, The Cryosphere, 8, 1393-1405, 2014.

Gladstone, R. M., Warner, R. C., Galton-Fenzi, B. K., Gagliardini, O., Zwinger, T., and Greve, R.: Marine ice sheet model performance depends on basal sliding physics and sub-shelf melting, The Cryosphere, 11, 319-329, 2017.

Gong, Y., Zwinger, T., Cornford, S., Gladstone, R., SchÄFer, M., and Moore, J. C.: Importance of basal boundary conditions in transient simulations: case study of a surging marine-terminating glacier on Austfonna, Svalbard, Journal of Glaciology, doi: 10.1017/jog.2016.121, 2016. 1-12, 2016.

Gudmundsson, G. H.: Ice-shelf buttressing and the stability of marine ice sheets, The Cryosphere, 7, 647-655, 2013.

Gudmundsson, G. H., Krug, J., Durand, G., Favier, L., and Gagliardini, O.: The stability of grounding lines on retrograde slopes, The Cryosphere, 6, 1497-1505, 2012.

Hoffman, M. and Price, S.: Feedbacks between coupled subglacial hydrology and glacier dynamics, Journal of Geophysical Research: Earth Surface, 119, 414-436, 2014.

Hoffman, M. J., Catania, G. A., Neumann, T. A., Andrews, L. C., and Rumrill, J. A.: Links between acceleration, melting, and supraglacial lake drainage of the western Greenland Ice Sheet, Journal of Geophysical Research: Earth Surface, 116, n/a-n/a, 2011.

Jenkins, A.: Convection-Driven Melting near the Grounding Lines of Ice Shelves and Tidewater Glaciers, Journal of Physical Oceanography, 41, 2279-2294, 2011.

Korona, J., Berthier, E., Bernard, M., Rémy, F., and Thouvenot, E.: SPIRIT. SPOT 5 stereoscopic survey of Polar Ice: Reference Images and Topographies during the fourth International Polar Year (2007–2009), ISPRS Journal of Photogrammetry and Remote Sensing, 64, 204-212, 2009.

Morlighem, M., Rignot, E., Seroussi, H., Larour, E., Ben Dhia, H., and Aubry, D.: A mass conservation approach for mapping glacier ice thickness, Geophysical Research Letters, 38, n/a-n/a, 2011.

Morlighem, M., Seroussi, H., Larour, E., and Rignot, E.: Inversion of basal friction in Antarctica using exact and incomplete adjoints of a higher-order model, Journal of Geophysical Research: Earth Surface, 118, 1746-1753, 2013.

Rignot, E., Casassa, G., Gogineni, S., Kanagaratnam, P., Krabill, W., Pritchard, H., Rivera, A., Thomas, R., Turner, J., and Vaughan, D.: Recent ice loss from the Fleming and other glaciers, Wordie Bay, West Antarctic Peninsula, Geophysical Research Letters, 32, 2005.

Rignot, E., Mouginot, J., Morlighem, M., Seroussi, H., and Scheuchl, B.: Widespread, rapid grounding line retreat of Pine Island, Thwaites, Smith, and Kohler glaciers, West Antarctica, from 1992 to 2011, Geophysical Research Letters, 41, 3502-3509, 2014.

Rignot, E., Mouginot, J., and Scheuchl, B.: Antarctic grounding line mapping from differential satellite radar interferometry, Geophysical Research Letters, 38, L10504, 2011a.

Rignot, E., Mouginot, J., and Scheuchl, B.: MEaSUREs InSAR-Based Antarctica Ice Velocity Map [Version1.0], Boulder, Colorado USA: NASA DAAC at the National Snow and Ice Data Center., doi: 10.5067/MEASURES/CRYOSPHERE/nsidc-0484.001, 2011b. 2011b.

Schoof, C.: Ice sheet grounding line dynamics: Steady states, stability, and hysteresis, Journal of Geophysical Research: Earth Surface, 112, n/a-n/a, 2007.

Schoof, C.: Ice-sheet acceleration driven by melt supply variability, Nature, 468, 803-806, 2010.

Sergienko, O., Creyts, T. T., and Hindmarsh, R.: Similarity of organized patterns in driving and basal stresses of Antarctic and Greenland ice sheets beneath extensive areas of basal sliding, Geophysical Research Letters, 41, 3925-3932, 2014.

Steiger, N., Nisancioglu, K. H., Åkesson, H., de Fleurian, B., and Nick, F. M.: Non-linear retreat of Jakobshavn Isbræ since the Little Ice Age controlled by geometry, The Cryosphere Discuss., 2017, 1-27, 2017.

Turner, J., Orr, A., Gudmundsson, G. H., Jenkins, A., Bingham, R. G., Hillenbrand, C.-D., and Bracegirdle, T. J.: Atmosphere-ocean-ice interactions in the Amundsen Sea Embayment, West Antarctica, Reviews of Geophysics, 55, 235-276, 2017.

Vaughan, D. G. and Doake, C. S. M.: Recent atmospheric warming and retreat of ice shelves on the Antarctic Peninsula, 1996. 1996.

Walker, C. C. and Gardner, A. S.: Rapid drawdown of Antarctica's Wordie Ice Shelf glaciers in response to ENSO/Southern Annular Mode-driven warming in the Southern Ocean, Earth and Planetary Science Letters, 476, 100-110, 2017.

Wendt, J., Rivera, A., Wendt, A., Bown, F., Zamora, R., Casassa, G., and Bravo, C.: Recent ice-surface-elevation changes of Fleming Glacier in response to the removal of the Wordie Ice Shelf, Antarctic Peninsula, Annals of Glaciology, 51, 97-102, 2010.

Wouters, B., Martin-Español, A., Helm, V., Flament, T., van Wessem, J. M., Ligtenberg, S. R. M., van den Broeke, M. R., and Bamber, J. L.: Dynamic thinning of glaciers on the Southern Antarctic Peninsula, Science, 348, 899-903, 2015.

Zhao, C., Gladstone, R., Zwinger, T., Warner, R., and King, M. A.: Basal drag of Fleming Glacier, Antarctica, Part 1: sensitivity of inversion to temperature and bedrock uncertainty, The Cryosphere, companion paper. companion paper.

Zhao, C., King, M. A., Watson, C. S., Barletta, V. R., Bordoni, A., Dell, M., and Whitehouse, P. L.: Rapid ice unloading in the Fleming Glacier region, southern Antarctic Peninsula, and its effect on bedrock uplift rates, Earth and Planetary Science Letters, 473, 164-176, 2017.

The Cryosphere Discuss., https://doi.org/10.5194/tc-2017-242
Manuscript under review for journal The Cryosphere
Discussion started: 2 January 2018

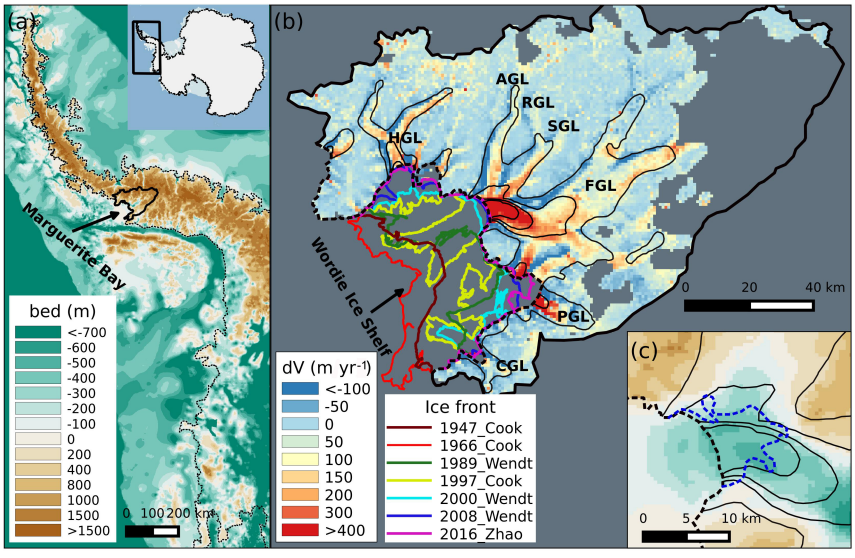

Figure 1. (a) The location of the study region in the Antarctica Peninsula (solid line polygon) with bedrock elevation data "bed_zc" ", based on BEDMAP2 (Fretwell et al., 2013) but refined using a mass conservation method for the fast-flowing regions of the Fleming Glacier system (Zhao et al., companion paper). (b) Velocity changes of the Wordie Ice Shelf-Fleming Glacier system from 2008 (Rignot et al., 2011b) to 2015 (Gardner et al., 2017). Black contours representing the velocity in 2008 with a spacing of 500 m yr^{-1}. The colored lines represent the ice front position in 1947, 1966, 1989, 1997, 2000, 2008, and 2016 obtained from Cook and Vaughan (2010), Wendt et al. (2010), and Zhao et al. (2017). The feeding glaciers for the Wordie Ice Shelf include three branches: Hariot Glacier (HGL) in the north, Airy Glacier (AGL), Rotz Glacier (RGL), Seller Glacier (SGL), Fleming Glacier (FGL), southern branch of the FGL (sFGL) in the middle, and Prospect Glacier (PGL), and Carlson Glacier (CGL) in the south. The grey area inside the catchment shows the region without velocity data. (c) Inset map of the Fleming Glacier with grounding line in 1996 (dashed black line) from Rignot et al. (2011a) and deduced grounding line in 2014 (dashed blue line) from Friedl et al. (2017). The background image is the bedrock from panel (a) and the black contours are same with panel (b).

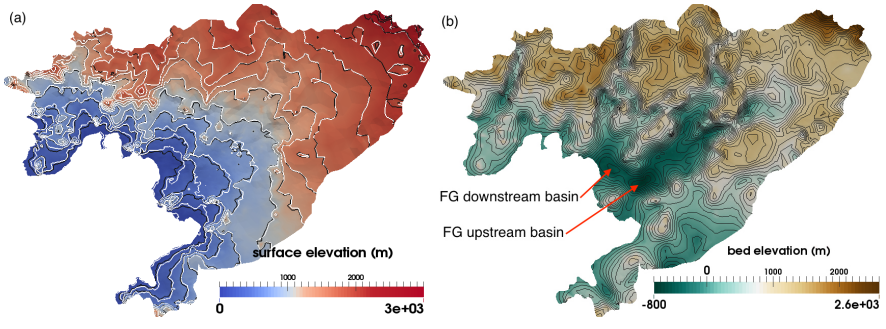

Figure 2. (a) Surface elevation data in 2008 (color scale) with black and white contours (interval: 200 m) representing the surface elevation in 2008 and 2015, respectively. (b) bed elevation data "bed_zc" with two basins "FGL downstream basin" and "FGL upstream basin" from Zhao et al. (companion paper). The black contours show the bed elevation with an interval of 100 m.

The Cryosphere Discuss., https://doi.org/10.5194/tc-2017-242
Manuscript under review for journal The Cryosphere
Discussion started: 2 January 2018

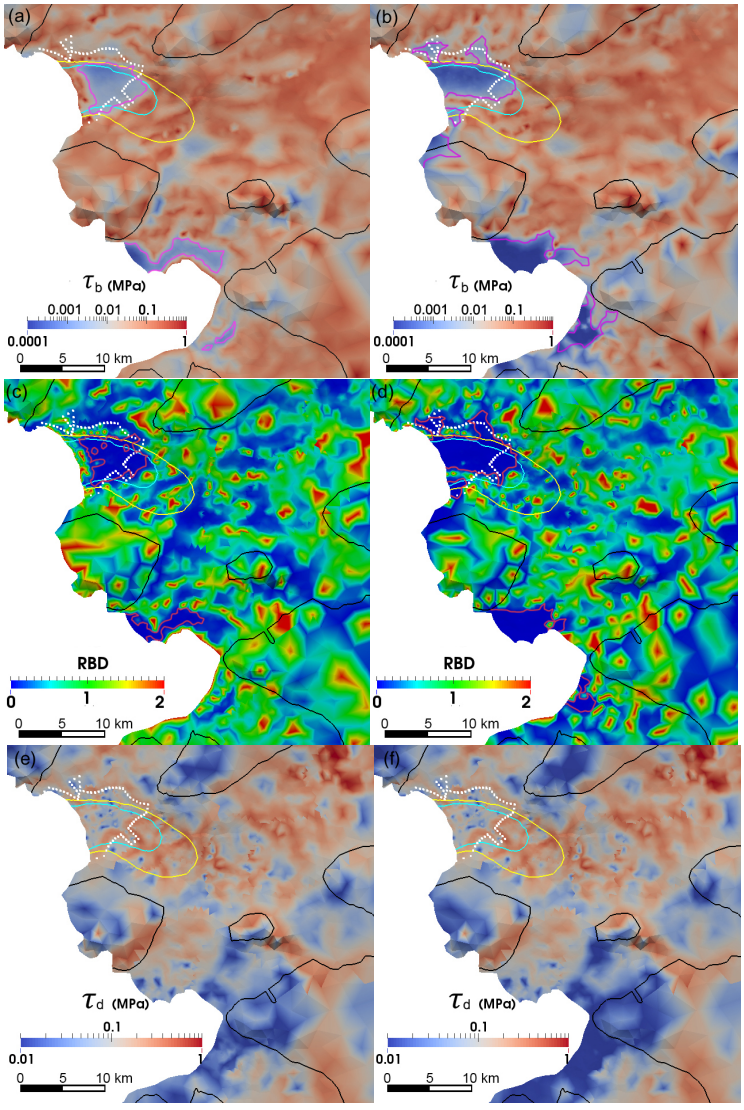

Figure 3. (a,b) Basal shear stress τ_b, (c, d) the ratio of τ_b to τ_d, and (e, f) the driving stress τ_d of the Fleming Glacier and the Prospect Glacier in 2008 (left) and 2015 (right). The white dotted line represents the deduced grounding line in 2014 from Friedl et al. (2017). The magenta lines in (a) and (b) shows the boundaries of selected area with τ_b<0.01 MPa in each simulation. The red lines in (c) and (d) show the boundaries of selected area with RBD < 0.1 in current study. The black, yellow and cyan solid lines represent the 2008 surface speed contours of 100 m yr^{-1}, 1000 m yr^{-1}, and 1500 m yr^{-1}, respectively, to give additional spatial connections between the figures.

The Cryosphere Discuss., https://doi.org/10.5194/tc-2017-242
Manuscript under review for journal The Cryosphere
Discussion started: 2 January 2018

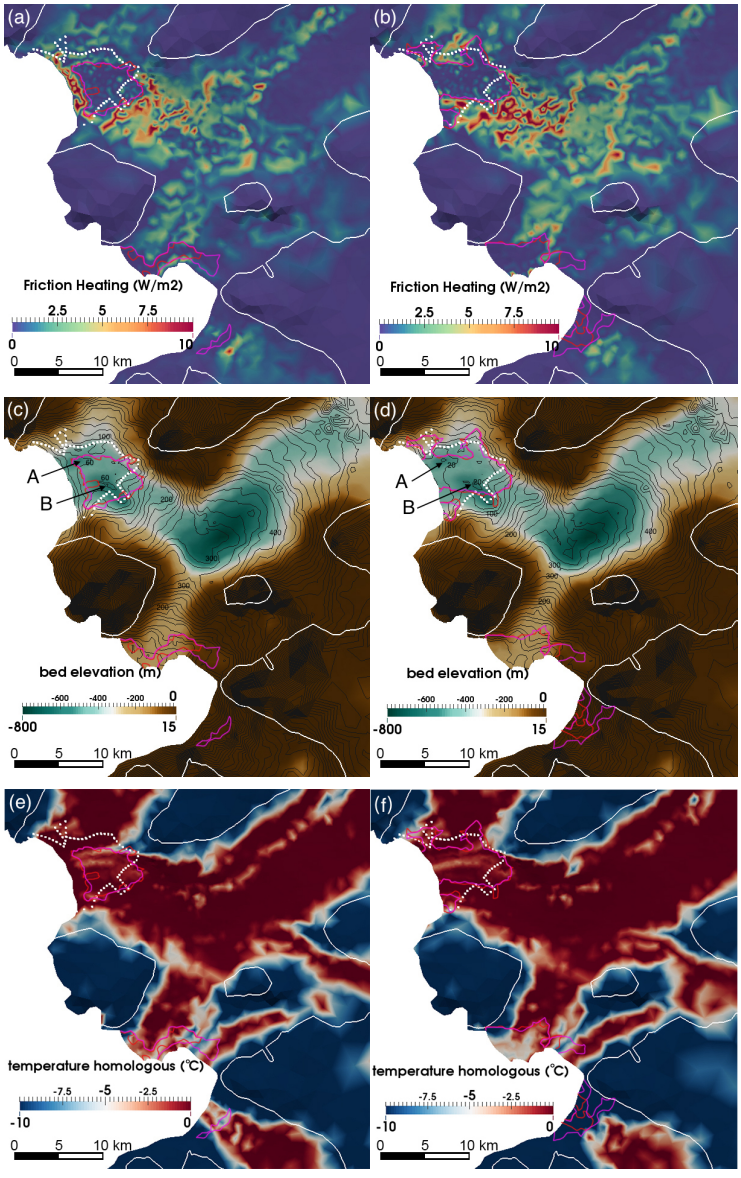

Figure 4. (a, b) The basal friction heating, (c, d) the contours of hydraulic potential with a spacing of 20 m with the bed elevation as the background, and (e, f) the simulated homologous temperature (temperature relative to the melting point) at the base of the Fleming Glacier and the Prospect Glacier in 2008 (left) and 2015 (right). The white dotted line represents the deduced grounding line in 2014 from Friedl et al. (2017). The white solid line represents the 2008 surface speed contours of 100 m yr^{-1}. The magenta and red solid lines show the boundaries of area with τ_b < 0.01 MPa and area with RBD < 0.1, respectively. A and B indicate the location of two over-deepened regions in the downstream basin.

The Cryosphere Discuss., https://doi.org/10.5194/tc-2017-242
Manuscript under review for journal The Cryosphere
Discussion started: 2 January 2018

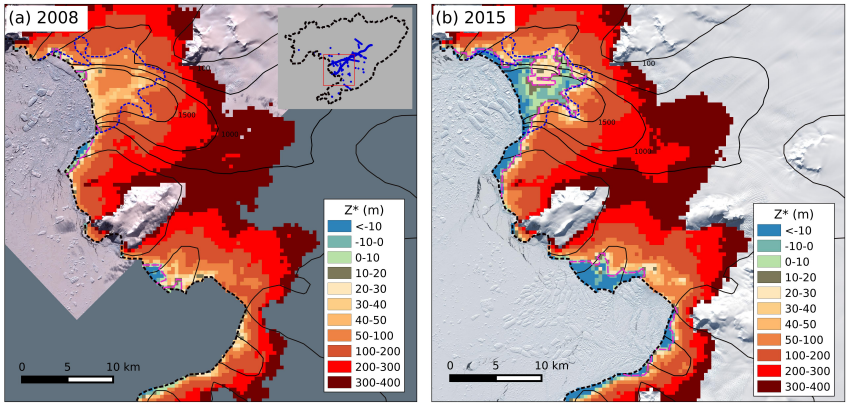

Figure 5. The height above buoyancy Z_* in (a) 2008 and (b) 2015 of the Fleming Glacier and Prospect Glacier. The background images are from (a) ASTER L1T data in Feb 2nd, 2009, and (b) Landsat-8 in Jan 13th 2016, respectively. The black lines represent velocity contours in 2008 (Rignot et al., 2011b) and 2015 (Gardner et al., 2017). The dashed black and blue lines show the grounding line in 1996 (Rignot et al., 2011a) and 2014 (Friedl et al., 2017), respectively. The dashed magenta line shows the possible grounding line with $Z_* < 20$ m. Inset map shows the location in the research domain with blue points showing the available elevation data points used to extract the hypsometric model of elevation change from 2008 to 2015 (Zhao et al., 2017).

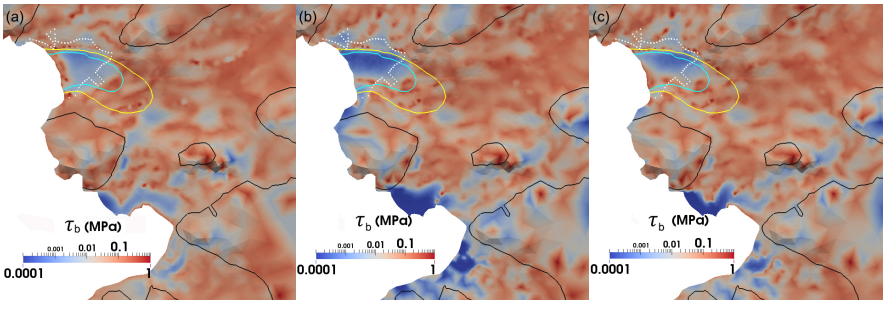

Figure A1. Basal shear stress, τ_b, for (a) 2008, (b) 2015, and (c) a simulation using topography from 2008 and velocity from 2015. The white dotted line represents the grounding line in 2014 estimated by Friedl et al. (2017). The black, yellow and cyan solid lines represent the 2008 surface speed contours of 100 m yr^{-1}, 1000 m yr^{-1}, and 1500 m yr^{-1}, respectively.